Chemical Engineering Journal 162 (2010) 521–527

Contents lists available at ScienceDirect

Chemical Engineering Journal

journal homepage: www.elsevier.com/locate/cej

Equilibrium, thermodynamic and kinetic studies on adsorption of Sb(III) from aqueous solution using low-cost natural diatomite

Ahmet Sarı*, Demirhan Çıtak, Mustafa Tuzen*

Department of Chemistry, Gaziosmanpasa University, 60250 Tokat, Turkey

ARTICLE INFO

Article history:
Received 26 April 2010
Received in revised form 24 May 2010
Accepted 26 May 2010

Keywords:
Diatomite
Antimony
Adsorption
Equilibrium
Thermodynamics
Kinetics

ABSTRACT

The equilibrium, thermodynamics and kinetics of antimony(III) adsorption from aqueous solution using low-cost natural diatomite were investigated using batch adsorption parameters such as pH and ionic strength. Langmuir, Freundlich and Dubinin–Radushkevich (D–R) isotherm models were applied to describe the isotherm models. The maximum adsorption capacity of diatomite for Sb(III) was found to be 35.2 mg/g at pH 6. The percent Sb(III) adsorbed in the presence of 0.001 M $NaNO_3$ at pH 6 was 68%, compared to 56 and 48% and at the same pH but in the presence of 0.01 and 0.1 M $NaNO_3$, respectively. From the D–R model, the mean adsorption energy was calculated as 7.32 kJ/mol, indicating that the adsorption of Sb(III) onto diatomite was physically carried out. The high stability of diatomite permitted a slightly decrease as about 10% in desorption yield and about 3% in adsorption yield after ten times of adsorption/desorption cycles. The calculated thermodynamic parameters (ΔG°, ΔH° and ΔS°) showed that the adsorption of Sb(III) onto diatomite was feasible, spontaneous and exothermic. Evaluation of the experimental data in terms of adsorption kinetics revealed that the adsorption of Sb(III) onto diatomite followed well the pseudo-second-order kinetic model.

1. Introduction

Heavy metal ions as inorganic pollutants, form a major class of environment contaminants [1,2]. Most heavy metals are known to be toxic and carcinogenic agents and, when discharged in wastewater, represent a serious threat to the human population. Many industries regarding with raw materials discharge of such metals into aquatic bodies and sources of drinking water has begun to be strictly controlled [3].

Antimony is one of the toxic metals and has much concern in terms of toxicological and environmental. Antimony has been extensively used in lead alloys, battery grids, bearing metal, cable sheathing, plumber's solder, pewter, ammunition, sheet and pipe. Among the most important uses of antimony in nonmetal products are textiles, paints and lacquers, rubber compounds, ceramic enamels, glass and pottery abrasives phosphorus (a beryllium replacement), and certain types of matches [$SbCl_3$] [4]. Because of the implication of antimony in cancer development [5], its compounds are considered to be pollutants of priority interest by the United States Environmental Protection Agency (USEPA) [6] and the European Union (EU) [7]. The World Health Organization (WHO) guidelines the antimony concentration as 0.005 mg/L in drinking waters [8]. The toxicological effects of antimony depend on its chemical form and oxidation state. The most favored form of antimony in water is the pentavalent antimonate oxoanion [$Sb(OH)_6^-$], while its other common inorganic form is antimonite [$Sb(OH)_3$] [9]. The Sb(III) form is ten times more toxic than Sb(V) form [10].

The monitoring and subsequent removal of antimony from aqueous solution has been compulsory due to its toxicological effects [11]. A number of methods have been used for the removal of antimony. These include reduction and precipitation [12], solvent extraction [13], ion exchange [14], reverse osmosis [15], membrane filtration [16], sorption in fixed-bed column [17] and biosorption [18,19].

On the other hand, adsorption method is more effective in reducing toxic metal concentration [20–24]. The adsorption systems have many advantages of simplicity, fastness and suitability for water and wastewater containing moderate and low concentrations of metals. Moreover, adsorbents must have a large surface area; a chemical nature and polarity of the adsorbent surface influence the attractive forces between the adsorbent and adsorbate [25]. A few studies on the use of adsorption method in the antimony removal process have been carried out [26–29].

Diatomite ($SiO_2 \cdot nH_2O$) or diatomaceous earth is a siliceous rock made up largely from the skeletons of aquatic plants called diatoms [30]. Diatomite is a pale-colored, soft, light-weight sedimentary rock composed principally of silica microfossils of aquatic unicellular algae. It has a unique combination of physical and chemical

* Corresponding authors. Tel.: +90 356 252 16 16; fax: +90 356 252 15 85.
E-mail addresses: asari@gop.edu.tr (A. Sarı), mtuzen@gop.edu.tr (M. Tuzen).

1385-8947/$ – see front matter © 2010 Elsevier B.V. All rights reserved.
doi:10.1016/j.cej.2010.05.054

properties such as high porosity, high permeability, small particle size, large surface area, and low thermal conductivity, which makes diatomite suitable for a wide range of industrial applications such as a filter aid or a filter [31]. Therefore, diatomite has been successfully used as adsorbent for different heavy metals removal from wastewaters [32–34].

Diatomite is abundantly available in Turkey markets and this could make it a strong candidate as an economical adsorbent for removing heavy metals from aqueous solutions. According to the authors' survey, there is no study regarding the adsorption of Sb(III) using diatomite in the literature. In this regard, the present work focused on the investigation of potential of diatomite for removal of Sb(III) from aqueous solution and optimization of conditions for its maximum adsorption. The equilibrium adsorption data were applied to the Langmuir, Freundlich and Dubinin–Radushkevich (D–R) isotherm models. The adsorption mechanism was also investigated in terms of thermodynamics and kinetics.

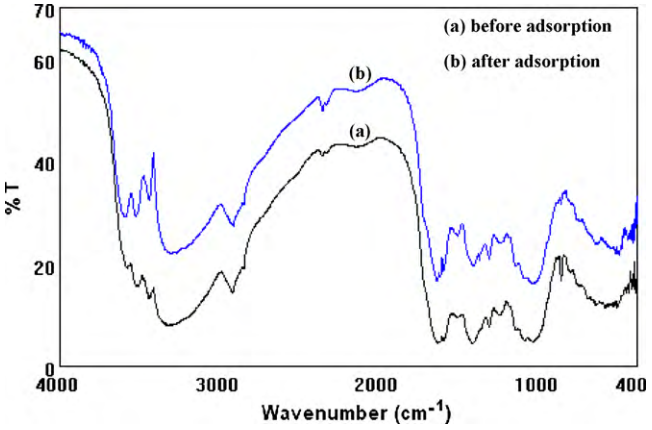

Fig. 1. FT-IR spectrum of adsorbent before and after adsorption.

2. Experimental procedures

2.1. Adsorbent and reagents

The diatomaceous earth was obtained from BEG-TUG Industrial Minerals & Mines Company (İstanbul, Turkey). The mineralogical composition of the dried sample supplied by the company is 92.8% SiO_2, 4.2% Al_2O_3, 0.3% MgO, 1.5% Fe_2O_3, 0.6% CaO, and 0.5% other oxides. In addition, all chemicals in this work were of analytical reagent grade and used without further purification. The structure of the sample is quite similar to that is analyzed by XRD analysis and reported by Sheng et al. [35]. The average pore size for the diatomite sample is with a wide distribution of pore size and micropore is dominant of the total pore volume of the diatomite [35].

2.2. Batch adsorption procedure

Sb(III) standard solution (1000 mg/L) was prepared from $SbCl_3$ (E. Merck, Darmstadt, Germany). Sodium phosphate buffer (0.1 mol/L) was prepared by adding an appropriate amount of phosphoric acid to sodium dihydrogen phosphate solution to result in a solution of pH 2–4. Ammonium acetate buffers (0.1 mol/L) were prepared by adding an appropriate amount of acetic acid to ammonium acetate solutions to result in solutions of pH 4–6. Ammonium chloride buffer solutions (0.1 mol/L) were prepared by adding an appropriate amount of ammonia to ammonium chloride solutions to result in solutions of pH 6–8. The adsorbent was then added and content in the flask was shaken for desired contact time on an electrically thermostatic reciprocating shaker (Selecta multimatic-55, Spain) at 120 rpm. The time required for reaching the adsorption equilibrium condition was estimated by drawing samples at regular intervals of time until equilibrium was reached. The contents of the flask were filtered through filter paper and the filtrate was analyzed for antimony concentration using AAS system (Perkin Elmer Analyst 700 model Norwalk, CT, USA) equipped with MHS 15 HGAAS system. A hallow cathode lamp operating at 15 mA was used and a spectral bandwidth of 0.7 nm was selected to isolate the 231.2 nm antimony line. $NaBH_4$ (1.5%) (w/v) in NaOH (0.5%) (w/v) was used as reducing agent. The analytical measurement was based on peak height. Reading time and argon flow rate was selected as 20 s and 70 mL min^{-1}.

The batch adsorption procedure mentioned above were repeated at different experimental parameters: the contact time 5–90 min, pH 2–10, initial metal concentration 10–400 mg/L, the adsorbent concentration 1–20 g/L and the temperature 20–50 °C. In addition, in order to investigate the effect of ionic strength on the adsorption of Sb(III) ions onto diatomite the electrolyte solutions at three different concentrations, 0.001 M $NaNO_3$, 0.01 M $NaNO_3$ and 0.1 M $NaNO_3$ were prepared.

All batch experiments were carried out in duplicated to ensure the accuracy, reliability and reproducibility of the collected data. The error bars and were also shown in the presentation of the results. The percent adsorption of Sb(III) was calculated as follows:

$$\text{Adsorption } (\%) = \frac{(C_i - C_f)}{C_i} \times 100 \quad (1)$$

where C_i (mg/L) and C_f (mg/L) are the initial and final Sb(III) concentrations, respectively.

2.3. Reusability test procedure

In order to the repeated availability of diatomite for Sb(III) adsorption, a reusability test consist of ten cycles of adsorption/desorption were carried out using 10 mL of 0.5 M HCl. After each adsorption/desorption cycle, antimony content of the solution was determined by HGAAS. In order to use the adsorbent for the next experiment, it was washed with excess of 0.5 M HCl solution and distilled water, sequentially.

3. Results and discussion

3.1. FT-IR analysis

The FT-IR spectra of diatomite were taken before and after adsorption by JASCO-430 model spectrophotometer in order to obtain information on the nature of probable interactions between the functional groups on the surface diatomite and antimony ions. The results are shown in Fig. 1. The broad bands observed at 3295, 3436, 3511, and 3577 cm^{-1} are due to the stretching vibration of the Si–OH and Al–OH groups. The spectral bands at 1600 and 1641 cm^{-1} reflect the bending vibration of water molecules retained in the silica or alumina matrix of diatomite. The peaks at 1041, 1105 and 470 cm^{-1} may be defined as asymmetric stretching modes of Si–O–Si bond. The peaks at 875 cm^{-1} may be attributed to the stretching vibration of Al–O–Si.

After adsorption of Sb(III) onto diatomite, the O–H stretching vibration of the Si–OH and Al–OH groups were observed at 3286, 3440, 3523, and 3592 cm^{-1}. The bending vibration of water molecules was observed at 1604 and 1647 cm^{-1}. The asymmetric stretching modes of Si–O–Si bond were shifted to 1051, 1105 and 474 cm^{-1} and the stretching vibration of Al–O–Si was shifted to 877 cm^{-1}. These small shifts in the wave number of specific bands indicated that the Si–OH and Al–OH groups on the surface of diatomite mainly involved in the adsorption of Sb(III). However,

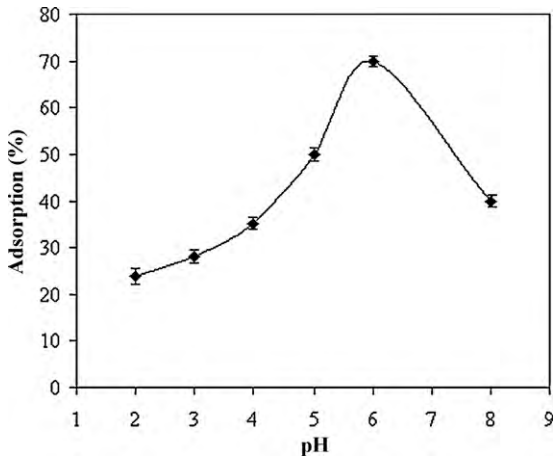

Fig. 2. Effect of pH on the adsorption of Sb(III) using diatomite (antimony concentration: 10 mg/L; temperature: 20 °C).

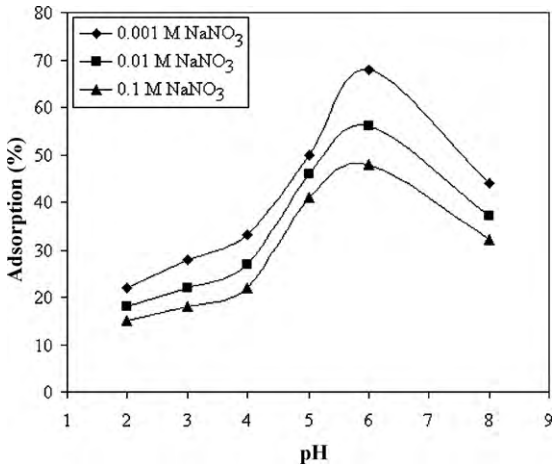

Fig. 3. Effect of ionic strength on the adsorption of Sb(III) using diatomite (antimony concentration: 10 mg/L; adsorbent concentration: 4 g/L; contact time: 30 min; temperature: 20 °C).

the adsorption may be carried out by weak physical attraction as electrostatic repulsion between the negative charges (Si–O$^-$ and Al–O$^-$) onto diatomite and antimony ions with positive charge.

3.2. Effect of pH

The pH parameter is one of the more important factors affecting adsorption process [36,37]. The effect of pH on the adsorption of Sb(III) onto diatomite was studied at pH 2–8, metal concentration 10 mg/L, adsorbent concentration 4 g/L, and temperature 20 °C. The results are presented in Fig. 2. In aqueous solution Sb(III) is available as $[SbO]^+$ and $[Sb(OH)_2]^+$ species at pH < 3. $[HSbO_2]$ and $[Sb(OH)_3]$ species are predominant at pH 3–10 and $[SbO_2]^-$ species are existing in aqueous solution at pH > 10 [11,38]. In the present work, the highest sorption (70%) was achieved at pH 6 while the adsorption yield was 24% at pH 2 and 40% after pH 8. Therefore, pH 6 was selected as optimum pH for further experiments. At pH < 2–4, the lower adsorption yield can be due to the fact that the hydronium ions with positive charge is abundantly available and thus the competition for the binding to the surface of the sorbent between the hydronium ions and antimony species, $[SbO]^+$ and $[Sb(OH)_2]^+$. Decrease in adsorption at higher pH (pH > 6) can be attributed to the competition for the sorption sites between hydroxyl ions and predominant the anionic antimony species, $[SbO_2]^-$. The similar results were reported based on the Zeta potential measurements with increasing pH [35]. Moreover, at higher pH values decrease in adsorption efficiency is due to the formation of soluble hydroxylated complexes of the antimony and their competition with the active sites, and as a consequence, adsorption would decrease. Similar results have also been reported for the sorption of antimony on rice husks [4], metal-loaded saponified orange waste [11], goethite (α-FeOOH) [37] and activated alumina [39].

3.3. Effect of ionic strength

The effect of ionic strength on the adsorption of Sb(III) onto diatomite was conducted at different pH values using three $NaNO_3$ electrolyte solutions with the concentration of 0.001, 0.01 and 0.1 M. As seen from Fig. 3, the percent Sb(III) adsorbed in the presence of 0.001 M $NaNO_3$ at pH 6 is 68%, compared to 56% and 48% and at the same pH but in the presence of 0.01 and 0.1 M $NaNO_3$, respectively. This may be due to the following two reasons: (i) The effect of ionic strength on metal adsorption may be explained by the formation of outer-sphere complexes since Na^+ in the background electrolyte could compete with the metal ions adsorbed on the outer-sphere adsorption sites and reduced the adsorption, whereas Na^+ would not have competed for the inner-sphere sites [40,41]. (ii) The electrostatic attraction seems to be a significant mechanism, as indicated by the results where at high ionic strength, the increased amount of $NaNO_3$ can help to render the surface of the diatomite easily accessible to Sb(III) ions and hence decreasing the adsorption rate.

3.4. Adsorption isotherm models

Adsorption isotherms are used to express the surface properties and affinity of the adsorbent and can also be used to compare the adsorption capacities of the sorbents for pollutants in aqueous solutions. In this study, the three adsorption isotherm models, Langmuir, Freundlich and Dubinin–Radushkevich (D–R) isotherm were selected to fit the equilibrium data.

A basic assumption of the Langmuir theory is that sorption takes place at specific homogeneous sites within the sorbent. This model can be written in non-linear form [42].

$$q_e = \frac{q_m K_L C_e}{1 + K_L C_e} \quad (2)$$

where q_e is the equilibrium metal ion concentration on sorbent (mg/g), C_e is the equilibrium metal ion concentration in the solution (mg/L), q_m is the monolayer adsorption capacity of the sorbent (mg/g), and K_L is the Langmuir adsorption constant (L/mg) related with the free energy of adsorption. Non-linear regression analysis was carried out in SigmaPlot software (SigmaPlot 2001, SPSS Inc., USA) in order to determine K_L and q_m values.

Fig. 4 indicates the non-linear Langmuir isotherm plot and the standard error in the determination of the parameters. As seen from the figure, the coefficient of determination (R^2) was found to be 0.9913. This result indicates that the adsorption of the Sb(III) onto diatomite fitted well the Langmuir model. In other words, the sorption of antimony using diatomite was taken place at the functional groups/binding sites on the surface of the adsorbent, which is regarded as monolayer adsorption. The maximum adsorption capacity (q_m) of diatomite was found to be 35.2 mg/g. The K_L value was found as 9.52×10^{-3} L/mg. In addition, Table 1 presents the comparison of adsorption capacity of diatomite for antimony with that of various sorbents reported in the literature [11,26,38,43]. As seen from this table, the diatomite has important potential for the removal of Sb(III) from aqueous solution.

The Freundlich model assumes a heterogeneous adsorption surface and active sites with different energy. The Freundlich model

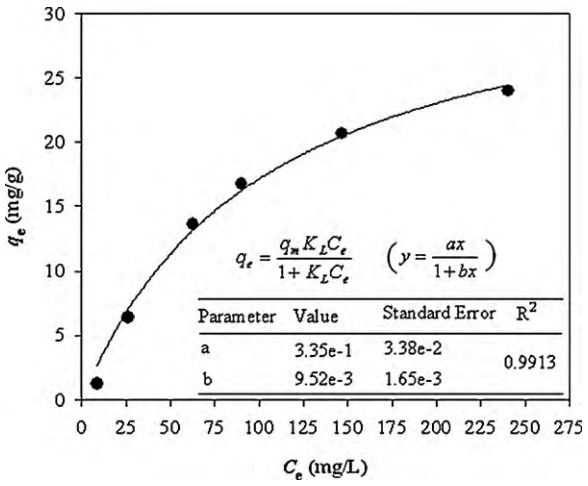

Fig. 4. Langmuir isotherm plots for the adsorption of Sb(III) onto diatomite (adsorbent concentration: 4 g/L; contact time: 30 min; pH 6; temperature: 20 °C).

Table 1
Comparison of Sb(III) sorption capacity of diatomite with that of different sorbents.

Sorbent	Sorption capacity (mg/g)	Reference
Zr(IV)-loaded SOW	114.49	[11]
Fe(III)-loaded SOW	136.42	[11]
Chemically bonded adsorbent	21.92	[26]
Goethite (α-FeOOH)	61.2 (average value)	[38]
Hydrous oxide of Mn	17.05	[43]
Hydrous oxide of Fe	12.18	[43]
Diatomite	35.2	Present study

[44] is

$$q_e = K_f C_e^{1/n} \quad (3)$$

where K_f is a constant relating the adsorption capacity and $1/n$ is an empirical parameter relating the adsorption intensity, which varies with the heterogeneity of the material.

Fig. 5 indicates the non-linear Freundlich isotherm plot and the standard error in the determination of the parameters. The K_f and $1/n$ values were found using non-linear regression analysis (SigmaPlot software, SigmaPlot 2001, SPSS Inc., USA). From the plot, K_f and $1/n$ values were found to be 1.25 and 0.55, respectively. The $1/n$ value were between 0 and 1 indicating that the adsorption of Sb(III) using diatomite was favorable at studied conditions. The

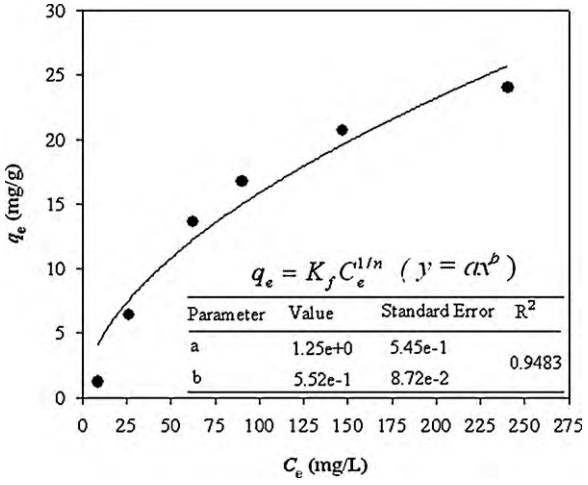

Fig. 5. Freundlich isotherm plots for the adsorption of Sb(III) onto diatomite (adsorbent concentration: 4 g/L; contact time: 30 min; pH 6; temperature: 20 °C).

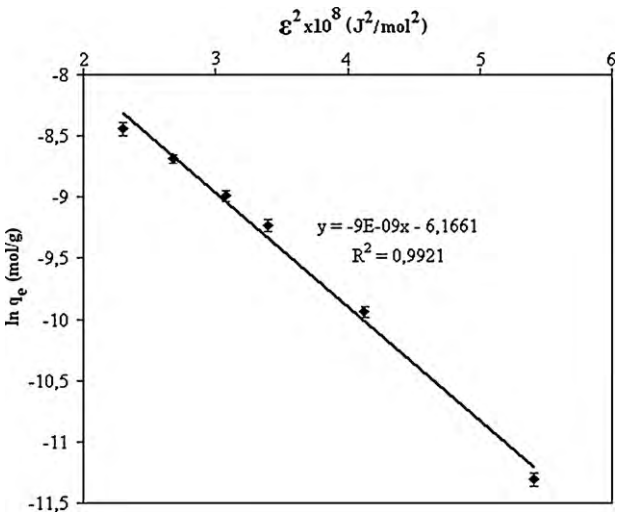

Fig. 6. D–R isotherm plots the adsorption of Sb(III) onto diatomite (adsorbent concentration: 4 g/L; contact time: 30 min; pH 6; temperature: 20 °C).

R^2 value was found to be 0.9483. This result means that that the Freundlich model was not able to adequately to describe the relationship between the amount of sorbed Sb(III) and its equilibrium concentration in the solution.

The equilibrium data were also applied to the D–R isotherm model to decide the nature of adsorption process as physical or chemical. The linear presentation of the D–R isotherm equation [45] is expressed by

$$\ln\ q_e = \ln\ q_m - \beta\varepsilon^2 \quad (4)$$

where q_e is the amount of metal ions sorbed on per unit weight of adsorbent (mol/L), q_m is the maximum adsorption capacity (mol/g), β is the activity coefficient related to mean free energy of adsorption (mol^2/J^2) and ε is the Polanyi potential ($\varepsilon = RT\ln(1 + 1/C_e)$).

The D–R isotherm model well fitted the equilibrium data since the R^2 value was found to be 0.9921 (Fig. 6). The q_m value was found using the intercept of the plot to be 2.1×10^{-3} mol/g. The mean free energy of adsorption (E, kJ/mol) is as follows:

$$E = \frac{1}{\sqrt{-2\beta}} \quad (5)$$

The E (kJ/mol) value gives information about sorption mechanism, physical or chemical in nature. The E value between 8 and 16 kJ/mol means that the sorption process takes place chemically when the values below 8 kJ/mol indicates it proceeds physically [46,47]. The mean free energy of adsorption was calculated to be 7.32 kJ/mol showing that the adsorption of Sb(III) onto diatomite was physical in nature.

3.5. Reusability

The repeated availability of diatomite for Sb(III) adsorption through many cycles of adsorption/desorption is quite crucial for the application of diatomite in the removal of Sb(III) from aqueous solution. The recycling of diatomite in the removal of Sb(III) was investigated. The high stability of diatomite permitted ten times of adsorption/desorption process along the studies with a decrease about 10% in desorption yield and about 3% in adsorption yield. Based on these results, it can be concluded that the diatomite was considered as good adsorbent with respect to the adsorption performance after a large number of sorption/desorption cycling.

Table 2
Kinetic parameters obtained from pseudo-first-order and pseudo-second-order at different temperatures.

Temperature (°C)	Pseudo-first-order				Pseudo-second-order		
	$q_{e,exp}$ (mg/g)	k_1 (1 min^{-1})	$q_{e1,cal}$ (mg/g)	R^2	k_2 (g/mg min)	$q_{e2,cal}$ (mg/g)	R^2
20	1.57	66.6×10^{-2}	0.953	0.943	26.3×10^{-2}	1.67	0.996
30	1.46	32.7×10^{-2}	0.942	0.902	25.2×10^{-2}	1.54	0.999
40	1.38	22.4×10^{-2}	0.934	0.945	24.1×10^{-2}	1.26	0.996
50	1.25	7.5×10^{-2}	0.912	0.912	22.8×10^{-2}	1.11	0.995

3.6. Adsorption kinetics

The prediction of adsorption rate is important for designing batch adsorption systems. In order to clarify the adsorption kinetics of Sb(III) onto diatomite, the Lagergren's pseudo-first-order and pseudo-second-order model were used to test the experimental data. The linear form of the pseudo-first-order rate equation by Lagergren [48] is given as

$$\ln(q_e - q_t) = \ln\ q_e - k_1 t \quad (6)$$

where q_t and q_e (mg/g) are the amounts of the metal ions biosorbed at equilibrium (mg/g) and t (min), respectively, and k_1 is the rate constant of the equation (min^{-1}). The adsorption rate constants (k_1) can be determined experimentally by plotting of $\ln(q_e - q_t)$ vs t. The R^2 and $q_{e,exp}$ values in Table 2 clearly indicated that the pseudo-first-order model is not suitable for modeling the adsorption of Sb(III) onto diatomite.

Experimental data were also tested by the pseudo-second-order kinetic model which is given in the following form [49]:

$$\frac{t}{q_t} = \frac{1}{k_2 q_e^2} + \left(\frac{1}{q_e}\right) t \quad (7)$$

where k_2 (g/mg min) is the rate constant of the second-order equation, q_t (mg/g) is the amount of adsorption time t (min) and q_e is the amount of adsorption equilibrium (mg/g). This model is more likely to predict kinetic behavior of adsorption [50]. The linear plots of t/q_t vs t for the pseudo-second-order model for the adsorption of Sb(III) onto diatomite at 20–50 °C are shown in Fig. 7. As seen from Table 2, the R^2 values are in range of 0.9952–0.9994 and the theoretical $q_{e2,cal}$ values were closer to the experimental $q_{e,exp}$ values. Based on these results, it can be concluded that the pseudo-second-order kinetic model provided a good correlation for the adsorption of Sb(III) onto diatomite in contrast to the pseudo-first-order model.

3.7. Adsorption thermodynamics

Thermodynamic parameters including the change in free energy (ΔG°), enthalpy (ΔH°) and entropy (ΔS°) were calculated from the following equations:

$$\Delta G^\circ = -RT\ \ln K_D \quad (8)$$

where R is the universal gas constant (8.314 J/mol K), T is the temperature (K) and K_D (q_e/C_e) is the distribution coefficient.

The enthalpy (ΔH°) and entropy (ΔS°) parameters were estimated from the following equation:

$$\ln K_D = \frac{\Delta S^\circ}{R} - \frac{\Delta H^\circ}{RT} \quad (9)$$

According to Eq. (9), the ΔH° and ΔS° parameters can be calculated from the slope and intercept of the plot of $\ln K_D$ vs $1/T$ yields, respectively (Fig. 8). The negative ΔH° (−18.53 kJ/mol) means that the adsorption process was carried out as exothermic at 20–50 °C. Furthermore, the negative ΔS° value (−9.65 kJ/mol K) indicates the decreased randomness at the solid–solution interface during the fixation of the antimony ion on the active sites of the adsorbent. Gibbs free energy change (ΔG°) was also calculated to be −15.67, −15.62, −15.53, and −15.37 kJ/mol for 20, 30, 40, and 50 °C, respectively. The negative ΔG° values indicated the spontaneous nature of the adsorption. These values (lower than −20.0 kJ mol^{-1}) indicate that electrostatic interaction may play a significant role in the adsorption process. It may be suggested that a surface complexation reaction is the major mechanism responsible for the Sb(III)

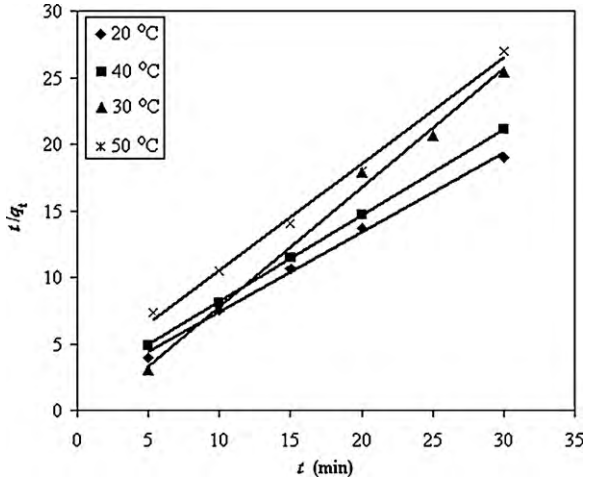

Fig. 7. Pseudo-second-order kinetic plots at different temperatures (metal concentration: 10 mg/L; pH 6; adsorbent concentration: 4 g/L).

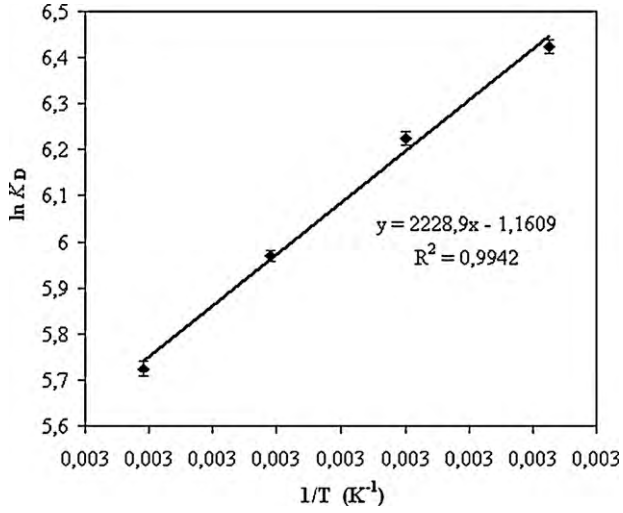

Fig. 8. Plot of $\ln K_D$ vs $1/T$ for the estimation of thermodynamic parameters the adsorption of Sb(III) onto diatomite (pH 6; adsorbent concentration: 4 g/L; contact time: 30 min).

adsorption process [51]. This conclusion was in good agreement with that obtained from the D–R isotherm model.

4. Conclusions

In this study, the equilibrium, thermodynamics and kinetics of the adsorption of Sb(III) from aqueous solution using low-cost natural diatomite were investigated using a batch system. The ionic strength and pH of solution were effective on the adsorption of Sb(III) onto diatomite. The maximum adsorption capacity of diatomite for Sb(III) was found to be 35.2 mg/g at pH 6. The percent Sb(III) adsorbed in the presence of 0.001 M $NaNO_3$ at pH 6 was 68%, compared to 56 and 48% and at the same pH but in the presence of 0.01 and 0.1 M $NaNO_3$, respectively. The calculated mean free energy (7.32 kJ/mol) indicated that the adsorption of Sb(III) using diatomite was physical in nature. The highest desorption yield (94%) was achieved using 0.5 M HCl. The high stability of using diatomite permitted a slightly decrease about 10% in desorption yield and about 3% in adsorption yield after ten times of adsorption/desorption process. The calculated thermodynamic parameters showed that the adsorption of Sb(III) onto using diatomite was feasible, spontaneous and exothermic under studied experimental conditions. The kinetic results revealed that the pseudo-second-order kinetic model provided the best description for the experimental data with coefficients of determination in range of 0.9952–0.9994. Furthermore, based on all results, it can be also concluded that the diatomite can be evaluated as an alternative adsorbent for the treatment of wastewater containing Sb(III) ions, due to its being low-cost adsorbent and having a considerable high sorption capacity.

Acknowledgements

The authors are grateful for the financial support of the Unit of the Scientific Research Projects of Gaziosmanpaşa University. The authors also would like to thank Assoc. Prof. Dr. Sedat Karaman for obtaining the diatomite sample.

References

[1] M.V. Dinu, E.S. Dragan, Evaluation of Cu^{2+}, Co^{2+} and Ni^{2+} ions removal from aqueous solution using a novel chitosan/clinoptilolite composite. Kinetics and isotherms, Chem. Eng. J. 160 (2010) 157–163.
[2] Y. Salameh, M.N.M. Ahmad, S.J. Allen, G.M. Walker, Kinetic and thermodynamic investigations on arsenic adsorption onto dolomitic sorbents, Chem. Eng. J. 160 (2010) 440–446.
[3] M.A. Al-Ghouti, M.A.M. Khraisheh, M. Tutuji, Flow injection potentiometric stripping analysis for study of adsorption of heavy metal ions onto modified diatomite, Chem. Eng. J. 104 (2004) 83–91.
[4] N. Khalid, S. Ahmad, A. Toheed, J. Ahmed, Potential of rice husks for antimony removal, Appl. Radiat. Isot. 52 (2000) 31–38.
[5] N. Gurnani, A. Sharma, G. Tulukder, Effects of antimony on cellular systems in animals: a review, Nucleus 37 (1994) 71–96.
[6] USEPA, Water Related Fate of the 129 Priority Pollutants, vol. 1, USEPA, Washington, DC, 1979 (Doc. 745-R-00-007).
[7] CEC (Council of the European Communities), Council Directive 6/substances discharged into aquatic environment of the community, Off. J. Eur. Commun. L129 (1976) 23–29.
[8] World Health Organization (WHO), Health criteria and other supporting information, in: Guidelines for Drinking-water Quality, vol. 2, 2nd ed., 1996, pp. 940–949.
[9] M. Fiella, N. Belzile, M.-C. Lett, Antimony in the environment: a review focused on natural waters. III. Microbiota relevant interaction, Earth-Sci. Rev. 80 (2007) 195–217.
[10] P. Smichowski, Y. Madrid, C. Camara, Analytical methods for antimony speciation in waters at trace and ultratrace levels. A review, Fresenius J. Anal. Chem. 360 (1998) 623–629.
[11] B.K. Biswas, J. Inoue, H. Kawakita, K. Ohto, K. Inoue, Effective removal and recovery of antimony using metal-loaded saponified orange waste, J. Hazard. Mater. 172 (2009) 721–728.
[12] K. Gannon, D.J. Wilson, Removal of antimony from aqueous solutions, Sep. Sci. Technol. 21 (1986) 475–493.
[13] W.M. Mok, C.M. Wai, Distribution and mobilization of arsenic and antimony species in the Coeur D'Alene River, Idaho, Environ. Sci. Technol. 24 (1990) 102–108.
[14] R. Guin, S.K. Das, S.K. Saha, The anion exchange behavior of Te and Sb, J. Radioanal. Nucl. Chem. Art. 230 (1998) 269–271.
[15] M. Kang, M. Kawasaki, S. Tamada, T. Kamei, Y. Magara, Effect of pH on the removal of the arsenic and antimony using reverse osmosis membranes, Desalination 131 (2000) 293–298.
[16] T. Saito, S. Tsuneda, A. Hirata, S. Nishiyama, K. Saito, K. Saito, K. Sugita, K. Uezu, M. Tamada, T. Sugo, Removal of antimony (III) using polyol-ligand-containing porous hollow-fiber membranes, Sep. Sci. Technol. 39 (2004) 3011–3022.
[17] A. Bakir, P. McLoughlin, S.A.M. Tofail, E. Fitzgerald, Competitive sorption of antimony with zinc, nickel, and aluminum in a seaweed based fixed-bed sorption column, Clean – Soil Air Water 37 (2009) 712–719.
[18] J. Tomko, M. Bačkor, M. Štofko, Biosorption of heavy metals by dry fungi biomass, Acta Metall. Slov. 12 (2006) 447–451.
[19] T. Perez-Corona, Y. Madrid, C. Camara, Evaluation of antimony selective uptake of selenium (Se(IV) and Se(V1)) and (Sb(III) and Sb(V)) species by baker's yeast cells (*Saccharomyces cerevisiae*), Anal. Chim. Acta 345 (1997) 249–255.
[20] K.G. Bhattacharyya, S. Sen Gupta, Influence of acid activation on adsorption of Ni(II) and Cu(II) on kaolinite and montmorillonite: kinetic and thermodynamic study, Chem. Eng. J. 136 (2008) 1–13.
[21] E. Demirbas, N. Dizge, M.T. Sulak, M. Kobya, Adsorption kinetics and equilibrium of copper from aqueous solutions using hazelnut shell activated carbon, Chem. Eng. J. 148 (2009) 480–487.
[22] G.D. Sheng, D.D. Shao, Q.H. Fan, Xu Di, Y.X. Chen, X.K. Wang, Effect of pH and ionic strength on sorption of Eu(III) to MX-80 bentonite: batch and XAFS study, Radiochim. Acta 97 (2009) 621–630.
[23] P. Chang, S. Yu, T. Chen, A. Ren, C. Chen, X. Wang, Effect of pH, ionic strength, fulvic acid and humic acid on sorption of Th(IV) on Na-rectorite, J. Radioanal. Nucl. Chem. 274 (2007) 153–160.
[24] V.C. Srivastava, I.D. Mall, I.M. Mishra, Adsorption thermodynamics and isosteric heat of adsorption of toxic metal ions onto bagasse fly ash (BFA) and rice husk ash (RHA), Chem. Eng. J. 132 (2007) 267–278.
[25] J. Li, J. Hu, G. Sheng, G. Zhao, Q. Huang, Effect of pH, ionic strength, foreign ions and temperature on the adsorption of Cu(II) from aqueous solution to GMZ bentonite, Colloid Surf. A: Physicochem. Eng. Aspects 349 (2009) 195–201.
[26] N.V. Deorkar, L.L. Tavlarides, A chemically bonded adsorbent for separation of antimony, copper and lead, Hydrometallurgy 46 (1997) 121–135.
[27] A Kathrinleuz, H. Mönch, C.A. Johnson, Sorption of Sb(III) and Sb(V) to goethite: influence on Sb(III) oxidation and mobilization, Environ. Sci. Technol. 40 (2006) 7277–7282.
[28] S.M. Hasany, M.H. Chaudhary, Sorption potential of haro river sand for the removal of antimony from acidic aqueous solution, Appl. Radiat. Isot. 47 (1996) 467.
[29] S. Imai, M. Muroi, A. Hamaguchi, R. Matsushita, M. Koyama, Preparation of dithiocarbamatecellulose derivatives and their adsorption properties for trace elements, Anal. Chim. Acta 113 (1980) 139–147.
[30] S. Akyuz, T. Akyuz, N.M. Ozer, FT-IR spectroscopic investigations of benzidine and bipyridyls adsorbed on diatomite from Anatolia, J. Mol. Struct. 565–566 (2001) 493–496.
[31] Y.S. Al-Degs, M.A.M.M. Khraisheh, M.F. Tutunji, Sorption of lead ions on diatomite and manganese oxides modified diatomite, Water Res. 35 (2001) 3724–3728.
[32] P. Moslehi, P. Nahid, Heavy metal removal from water and wastewater using raw and modified diatomite, IJE Trans. B: Appl. 20 (2007) 141–146.
[33] M.A.M.M. Khraisheh, Y.S. Al-Degs, W.A.M. Mcminn, Remediation of wastewater containing heavy metals using raw and modified diatomite, Chem. Eng. J. 99 (2004) 177–184.
[34] M.A. Al-Ghouti, M.A.M.M. Khraisheh, M. Tutuji, Flow injection potentiometric stripping analysis for study of adsorption of heavy metal ions onto modified diatomite, Chem. Eng. J. 104 (2004) 83–91.
[35] G. Sheng, S. Wang, J. Hu, Y. Lu, J. Li, Y. Dong, X. Wang, Adsorption of Pb(II) on diatomite as affected via aqueous solution chemistry and temperature, Colloid Surf. A: Physicochem. Eng. Aspects 339 (2009) 159–166.
[36] C. Chen, X. Wang, Sorption of Th(IV) to silica as a function of pH, humic/fulvic acid, ionic strength, electrolyte type, Appl. Radiat. Isot. 65 (2007) 155–163.
[37] A. Sari, D. Mendil, M. Tuzen, M. Soylak, Biosorption of Cd(II) and Cr(III) from aqueous solution by moss (*Hylocomium splendens*) biomass: equilibrium, kinetic and thermodynamic studies, Chem. Eng. J. 144 (2008) 1–9.
[38] R. Watkins, D. Weiss, W. Dubbin, K. Peel, B. Coles, T. Arnold, Investigations into the kinetics and thermodynamics of Sb(III) adsorption on goethite (α-FeOOH), J. Colloid Interface Sci. 303 (2006) 639–646.
[39] Y.-H. Xu, A. Ohki, S. Maeda, Adsorption and removal of antimony from aqueous solution by an activated alumina 1. Adsorption capacity of adsorbent and effect of process variable, Toxicol. Environ. Chem. 80 (2001) 133–144.
[40] X. Guo, S. Zhang, X.-Q. Shan, Adsorption of metal ions on lignin, J. Hazard. Mater. 151 (2008) 134–142.
[41] S. Yang, J. Li, Y. Yi Lu, X. Chen, Wang, Sorption of Ni(II) on GMZ bentonite: effects of pH, ionic strength, foreign ions, humic acid and temperature, Appl. Radiat. Isot. 67 (2009) 1600–1608.
[42] I. Langmuir, The adsorption of gases on plane surfaces of glass, mica and platinum, J. Am. Chem. Soc. 40 (1918) 1361–1403.
[43] P. Thanabalasingam, W.F. Pickering, Specific sorption of antimony(III) by the hydrous oxides of Mn, Fe and Al, Water Air Soil Pollut. 49 (1990) 175–185.

[44] H.M.F. Freundlich, Über die adsorption in lösungen, Z. Phys. Chem. (Leipzig) 57A (1906) 385–470.
[45] M.M. Dubinin, E.D. Zaverina, L.V. Radushkevich, Sorption and structure of active carbons. I. Adsorption of organic vapors, Zh. Fiz. Khim. 21 (1947) 1351–1362.
[46] R. Altun Anayurt, A. Sari, M. Tuzen, Equilibrium, thermodynamic and kinetic studies on biosorption of Pb(II) and Cd(II) from aqueous solution by macrofungus (*Lactarius scrobiculatus*) biomass, Chem. Eng. J. 151 (2009) 255–261.
[47] M. Tuzen, A. Sari, Biosorption of selenium from aqueous solution by green algae (*Cladophora hutchinsiae*) biomass: equilibrium, thermodynamic and kinetic studies, Chem. Eng. J. 158 (2010) 200–206.
[48] S. Lagergren, Zur theorie der sogenannten adsorption geloster stöffe, Kungliga Sevenska Vetenskapsakademiens, Handlingar 24 (1898) 1.
[49] Y.S. Ho, G. McKay, Pseudo-second order model for sorption processes, Process Biochem. 34 (1999) 451–465.
[50] Y.S. Ho, G. McKay, D.A.J. Wase, C.F. Forster, Study of the sorption of divalent metal ions on to peat, Ads. Sci. Technol. 18 (2000) 639–650.
[51] C.-H. Weng, C.-Z. Tsai, S.-H. Chu, Y.C. Sharma, Adsorption characteristics of copper(II) onto spent activated clay, Sep. Purif. Technol. 54 (2007) 187–197.